Bicocca-FT-00-20

Non–perturbative scaling tests of twisted mass QCD *

M. Della Morte[a], R. Frezzotti[a], J. Heitger[b] and S. Sint [c]

[a]Dipartimento di Fisica, Università di Milano–Bicocca and INFN Sezione di Milano, Milano, Italy

[b]Westfälische Wilhelms-Universität Münster, Institut für Theoretische Physik, Münster, Germany

[c]CERN, Theory Division, Geneva, Switzerland

We present a scaling study of lattice QCD with O(a) improved Wilson fermions and a chirally twisted mass term. In order to get precise results with a moderate computational effort, we have considered a system of physical size of $0.75^3 \times 1.5$ fm^4 with Schrödinger functional boundary conditions in the quenched approximation. Looking at meson observables in the pseudoscalar and vector channels, we find that O(a) improvement is effective and residual cutoff effects are fairly small.

1. Introduction

Twisted mass QCD (tmQCD) was introduced in [1] to solve the problem of unphysical fermion zero modes in lattice QCD with two degenerate flavours of Wilson fermions. The fermion lattice tmQCD action reads:

$$S_F = a^4 \sum_x \overline{\psi}(x) \left(D + m_0 + i\mu_{\rm q}\gamma_5\tau^3 \right) \psi(x) \;, \quad (1)$$

where D is the O(a) improved Wilson lattice regularization[1] of $\not{D}$ and $m_0 \equiv 1/2\kappa - 4$ and $\mu_{\rm q}$ are two real quark mass parameters. The lattice symmetries and power counting determine the counterterm structure for renormalization and O(a) improvement of the infinite volume theory. The physical equivalence of tmQCD to QCD in the continuum limit has been argued in [1] and will be further detailed in [3].

We study tmQCD in a four dimensional box with Schrödinger functional (SF) boundary conditions. We wish to check that after on-shell O(a) improvement à la Symanzik [4] a few renormalized quantities related to meson physics approach the continuum limit with residual scaling violations that are small and compatible with being O(a^2). Following ref. [7], we keep the spatial size of the box moderately small ($L \simeq 0.75$ fm) and choose $T = 2L$.

The transfer matrix of lattice tmQCD with action (1) and $c_{\rm SW} = 0$ can be constructed in close analogy to ref. [10] and turns out to be self-adjoint and strictly positive for $|\kappa| < 1/6$ [3]. Following refs. [8, 11], the Schrödinger functional in tmQCD can be conveniently defined as the integral kernel of an integer power T/a of the transfer matrix [3]. It has an Euclidean representation given by

$$\mathcal{Z}[\rho', \overline{\rho}', C'; \rho, \overline{\rho}, C] \;=\; \int_{\rm fields} e^{-S[U,\psi,\bar{\psi}]} \qquad (2)$$

and can hence be considered as a functional of the fields at the Euclidean times 0 and T. The structure of the transfer matrix implies that the boundary conditions for gauge and quark fields are the same as in the standard framework ($\mu_{\rm q} = 0$). The action $S[U, \bar{\psi}, \psi]$ in eq. (2) is the sum of the usual plaquette pure gauge action and the quark action, which takes the same form as in eq. (1), provided one adopts the notational conventions of Subsect. 4.2 of [2].

The tmQCD Schrödinger functional is expected to be finite after the standard couplings and boundary renormalization [3]. At order a new boundary counterterms proportional to $a\mu_{\rm q}$ arise [3]. Their effect beyond tree–level will be neglected in this study.

*Based on a poster by M. Della Morte presented at the International Symposium on Lattice Field Theory, August 2000, Bangalore, India.

[1]See ref. [2] for notation and details.

2. Correlation functions

In order to motivate our choice of observables, we recall some properties of renormalized tmQCD. For simplicity, we first consider the theory with boundary conditions that are periodic in space and as specified in [10] in time direction. The renormalization scheme (R) of tmQCD can be chosen [3] to be consistent with the Ward identities of the flavour chiral symmetries:

$$\begin{aligned} \partial_\mu (A_\mathrm{R})^a_\mu &= 2m_\mathrm{R}(P_\mathrm{R})^a + \delta^{a3} i\mu_\mathrm{R}(S_\mathrm{R})^0 \qquad (3) \\ \partial_\mu (V_\mathrm{R})^a_\mu &= -2\mu_\mathrm{R}\varepsilon^{ab3}(P_\mathrm{R})^b \qquad (4) \end{aligned}$$

where the above relations are to be understood as operator insertions[2] in the correlation functions and ε is fully antisymmetric with $\varepsilon^{123}=1$. Note that our chirally twisted parameterization of QCD involves two renormalized mass parameters, m_R and μ_R.

It can be shown [1, 3] that, within a certain subset of the renormalization schemes that preserve the above Ward identities, the *on-shell* correlation functions of tmQCD can be mapped onto the ones of standard QCD in a related renormalization scheme. In the latter scheme the flavour chiral Ward identities (at the operator level) read:

$$\partial_\mu (A_\mathrm{R})^a_\mu = 2m'_\mathrm{R}(P_\mathrm{R})^a \; , \qquad \partial_\mu (V_\mathrm{R})^a_\mu = 0 \qquad (5)$$

for $a=1,2,3$ with the mass m'_R satisfying:

$$(m'_\mathrm{R})^2 = m_\mathrm{R}^2 + \mu_\mathrm{R}^2 \; , \quad \tan(\alpha) = \mu_\mathrm{R}/m_\mathrm{R} \; . \qquad (6)$$

Here α is an unphysical angle which just specifies the quark mass parameterization. An example of this mapping is given by:

$$\begin{aligned} &\langle (A_\mathrm{R})^2_0(x)(P_\mathrm{R})^2(y)\rangle_\mathrm{c}\{g_\mathrm{R}, m'_\mathrm{R}, 0\} = \\ &\langle (A'_\mathrm{R})^2_0(x)(P'_\mathrm{R})^2(y)\rangle_\mathrm{c}\{g_\mathrm{R}, m_\mathrm{R}, \mu_\mathrm{R}\} \; , \qquad (7) \end{aligned}$$

where $x \neq y$ and by definition:

$$\begin{aligned} (A'_\mathrm{R})^a_\mu &= \cos(\alpha)(A_\mathrm{R})^a_\mu + \sin(\alpha)\varepsilon^{ab3}(V_\mathrm{R})^b_\mu \; , \\ (P'_\mathrm{R})^a &= (P_\mathrm{R})^a \qquad a=1,2 \; . \qquad (8) \end{aligned}$$

It is understood that in eq. (7) the l.h.s. must be evaluated at renormalized couplings $\{g_\mathrm{R}, m'_\mathrm{R}, 0\}$ and the r.h.s at renormalized couplings $\{g_\mathrm{R}, m_\mathrm{R}, \mu_\mathrm{R}\}$, with the quark mass couplings related via eq. (6). Note that the above mapping takes the same form as at the classical level, where it is obtained via [1]

$$\psi'_\mathrm{cl} = e^{i\alpha\gamma_5\tau^3/2}\psi_\mathrm{cl} \; , \qquad \bar\psi'_\mathrm{cl} = \bar\psi_\mathrm{cl} e^{i\alpha\gamma_5\tau^3/2} \; .$$

In the following we will also need to consider, again for $a=1,2$ only, the primed fields:

$$\begin{aligned} (V'_\mathrm{R})^a_\mu &= \cos(\alpha)(V_\mathrm{R})^a_\mu + \sin(\alpha)\varepsilon^{ab3}(A_\mathrm{R})^b_\mu \; , \\ (T'_\mathrm{R})^a_{\mu\nu} &= (T_\mathrm{R})^a_{\mu\nu} \qquad a=1,2 \; . \qquad (9) \end{aligned}$$

Coming back to our scaling tests of tmQCD with SF boundary conditions, we focus on a few renormalized quantities that can be extracted from the following correlators:

$$\begin{aligned} f^{22}_{\mathrm{R,A'}}(x_0) &= -\langle (A'_\mathrm{R})^2_0(x)\mathcal{O}^2_5\rangle / \sqrt{f_1^{22}} \; , \\ f^{22}_{\mathrm{R,P'}}(x_0) &= -\langle (P'_\mathrm{R})^2(x)\mathcal{O}^2_5\rangle / \sqrt{f_1^{22}} \qquad (10) \end{aligned}$$

and (with sum over $k=1,2,3$ understood)

$$\begin{aligned} k^{22}_{\mathrm{R,V'}}(x_0) &= -\frac{1}{3}\langle (V'_\mathrm{R})^2_k(x)\mathcal{Q}^2_k\rangle / \sqrt{f_1^{22}} \; , \\ k^{22}_{\mathrm{R,T'}}(x_0) &= -\frac{1}{3}\langle (T'_\mathrm{R})^2_{k0}(x)\mathcal{Q}^2_k\rangle / \sqrt{f_1^{22}} \; , \qquad (11) \end{aligned}$$

where $\mathcal{O}^a_5$ and $\mathcal{Q}^a_k$ are the SF boundary fields defined in ref. [7] at zero Euclidean time[3]. In the above correlators the division by the square root of the quantity

$$f_1^{22} = -\frac{1}{L^6}\langle {\mathcal{O}'}^2_5 \mathcal{O}^2_5\rangle \; , \qquad (12)$$

takes care of the boundary field renormalization.

In the quantum mechanical representation of the renormalized correlation functions that are obtained from eq. (10) and eq. (11), the only non–vanishing contributions (up to cutoff effects) arise when inserting states with vacuum quantum numbers at Euclidean times between x_0 and T, and states with pion and ρ–meson quantum numbers, respectively, at Euclidean times between 0 and x_0. Let us consider for instance the SF correlator $f^{22}_{\mathrm{R,A'}}$: the matrix elements between intermediate states $|k\rangle$ and $|n\rangle$

$$\langle k|\cos(\alpha)(A_\mathrm{R})^2_0 - \sin(\alpha)(V_\mathrm{R})^1_0|n\rangle \; , \qquad (13)$$

[2] The quark bilinears are defined in the standard way, with flavour matrices $\tau^a/2$ (for $a=1,2,3$) or $\tau^0=1$.

[3] The analogous fields localized on the other SF time-boundary are labelled with a prime.

which enter its quantum mechanical representation, are independent of the SF boundary conditions and also appear in the quantum mechanical representation of the r.h.s. of eq. (7). The equality of the correlators in eq. (7) implies the equality of their quantum mechanical representations for arbitrary values of $(x_0 - y_0)$. From this equality it follows that in tmQCD the matrix elements of the form (13) with the states $|k\rangle$ and $|n\rangle$ carrying vacuum and pion quantum numbers, respectively, are non-zero. Analogous arguments hold for the remaining SF correlators in eqs. (10)–(11). The fields $\mathcal{O}_5^a$ and $\mathcal{Q}_k^a$ are chosen so that the corresponding SF boundary states have a non–zero overlap with the pion and the ρ–meson states.

3. Definition of the observables

In this study we consider as observables some ratios of the previously introduced SF finite volume correlators that are expected to approach a well defined *continuum limit*[4]:

$$m_{\rm PS} = \frac{\tilde\partial_0 f^{22}_{\rm R,P'}(x_0)}{f^{22}_{\rm R,P'}(x_0)} , \quad x_0 = T/2 , \qquad (14)$$

$$\widetilde m_{\rm PS} = \frac{\tilde\partial_0 f^{22}_{\rm R,A'}(x_0)}{f^{22}_{\rm R,A'}(x_0)} , \quad x_0 = T/2 , \qquad (15)$$

$$m_{\rm V} = \frac{\tilde\partial_0 k^{22}_{\rm R,V'}(x_0)}{k^{22}_{\rm R,V'}(x_0)} , \quad x_0 = T/2 , \qquad (16)$$

$$\widetilde m_{\rm V} = \frac{\tilde\partial_0 k^{22}_{\rm R,T'}(x_0)}{k^{22}_{\rm R,T'}(x_0)} , \quad x_0 = T/2 , \qquad (17)$$

$$\eta_{\rm PS} = C_{\rm PS} f^{22}_{\rm R,A'}(x_0) , \quad x_0 = T/2 , \qquad (18)$$

$$\widetilde\eta_{\rm PS} = \widetilde C_{\rm PS} f^{22}_{\rm R,A'}(x_0) , \quad x_0 = T/2 , \qquad (19)$$

$$\eta_{\rm V} = C_{\rm V} k^{22}_{\rm R,V'}(x_0) , \quad x_0 = T/2 , \qquad (20)$$

$$\widetilde\eta_{\rm V} = \widetilde C_{\rm V} k^{22}_{\rm R,V'}(x_0) , \quad x_0 = T/2 . \qquad (21)$$

As $T = 2L \to \infty$, $m_{\rm PS}$ and $m_{\rm V}$ yield estimators of the pion and ρ-meson mass, respectively. The constants $C_{\rm PS}$ and $C_{\rm V}$ are defined as in [7] in terms of $m_{\rm PS}$ and $m_{\rm V}$. $C_{\rm PS}$ is such that $\eta_{\rm PS} \to F_\pi$ as $T = 2L \to \infty$. The quantity $\eta_{\rm V}$ is not related to the decay of the ρ–meson because of its unphysical normalization. Analogous considerations hold for the alternative scaling quantities labelled with a "tilde".

The $f_{\rm R}$- and $k_{\rm R}$ correlators entering our observables are defined in eqs. (10)–(12) via eqs. (8)–(9) and

$$\begin{aligned}
(A_{\rm R})^a_\mu &= Z_{\rm A}(1 + b_{\rm A} am_{\rm q})(A_{\rm I})^a_\mu , \\
(V_{\rm R})^a_\mu &= Z_{\rm V}(1 + b_{\rm V} am_{\rm q})(V_{\rm I})^a_\mu , \\
(P_{\rm R})^a &= Z_{\rm P}(1 + b_{\rm P} am_{\rm q})(P_{\rm I})^a , \\
(T_{\rm R})^a_{\mu\nu} &= Z_{\rm T}(1 + b_{\rm T} am_{\rm q})(T_{\rm I})^a_{\mu\nu} , \qquad (22)
\end{aligned}$$

where (restricting attention to $a = 1, 2$)

$$\begin{aligned}
(A_{\rm I})^a_\mu &= A^a_\mu + c_{\rm A} a\tilde\partial_\mu P^a + a\mu_{\rm q}\tilde b_{\rm A}\varepsilon^{ab3}V^b_\mu , \\
(V_{\rm I})^a_\mu &= V^a_\mu + c_{\rm V} a\tilde\partial_\nu T^a_{\mu\nu} + a\mu_{\rm q}\tilde b_{\rm V}\varepsilon^{ab3}A^b_\mu , \\
(P_{\rm I})^a &= P^a , \\
(T_{\rm I})^a_{\mu\nu} &= T^a_{\mu\nu} + c_{\rm T} a(\tilde\partial_\mu V^a_\nu - \tilde\partial_\nu V^a_\mu) . \qquad (23)
\end{aligned}$$

For the definition of the bare lattice fields A^a_μ, P^a, V^a_μ and $T^a_{\mu\nu}$ we follow Sect. 2 of ref. [9]. The suffix I refers to the O(a) improvement of these fields, which together with O(a) improvement of the action, eq. (1), implies that -in the limit $T \to \infty$- the observables in eqs. (14)–(21) deviate from their continuum limit by O(a^2) cutoff effects. The $\tilde b$ coefficients multiply counterterms that are needed to subtract (bulk) cutoff effects of order $a\mu_{\rm q}$.

4. Results

We choose non–perturbative *mass–independent* renormalization conditions for the couplings and the observables of interest. As L/a is increased, the relation between $\beta = 6/g_0^2$ and a/r_0 [12] is employed in order to keep the physical size of the box fixed at $L = 1.49 r_0$, with r_0 being a hadron scale of order 0.5 fm. The mass parameter κ is tuned so to keep fixed the PCAC renormalized mass in units of L:

$$Lm_{\rm R} \stackrel{\rm def}{=} \frac{L}{a}\left\{\frac{Z_{\rm A}}{Z_{\rm P}}\frac{\tilde\partial_0 f^{22}_{\rm A}}{2f^{22}_{\rm P}}\right\} = 0.020 , \qquad (24)$$

where:

$$\begin{aligned}
Z_{\rm A} f^{22}_{\rm A} &= -\langle (A_{\rm R})^2_0(x)\mathcal{O}^2_5\rangle , \\
Z_{\rm P} f^{22}_{\rm P} &= -\langle (P_{\rm R})^2(x)\mathcal{O}^2_5\rangle . \qquad (25)
\end{aligned}$$

[4] The symbol $\tilde\partial_\mu$ denotes the symmetric lattice derivative.

The mass parameter $\mu_{\rm q}$ is chosen so to fulfill the condition:

$$L\mu_{\rm R} \stackrel{\rm def}{=} Z_{\rm P}^{-1} L\mu_{\rm q} = 0.153 \; . \qquad (26)$$

This choice is justified by the exact *lattice* Ward identity $\partial_\mu^* \widetilde{V}_\mu^2 = 2\mu_{\rm q} P^1$, where $\widetilde{V}_\mu^a$ is the one–point split vector current that is conserved at $\mu_{\rm q} = 0$ and ∂_μ^* denotes the backward lattice derivative. The angle α, given by $\tan(\alpha) = \mu_{\rm R}/m_{\rm R}$, is close to $\pi/2$.

β	$\mu_{\rm q}$	κ	L/r_0	$Lm_{\rm R}$
6.0	0.01	0.134952	1.490(6)	0.0228(23)
6.14	0.00794	0.135614	1.486(7)	0.0203(30)
6.26	0.00659	0.135742	1.495(7)	0.0201(23)
6.47	0.00493	0.135611	1.488(7)	0.0180(24)

Table 1
The bare and renormalized parameters in our simulations. As for L/a and $L\mu_{\rm R}$ see the text.

The renormalization factors $Z_{\rm A}$, $Z_{\rm V}$ and $Z_{\rm P}$ were determined in [6] and [13], where $Z_{\rm P}$ is given as a function of β at the scale $L_0 = 1.436 r_0$. As for the improvement coefficients, we employ non–perturbative estimates of $c_{\rm SW}$, $c_{\rm A}$ [5] and $b_{\rm V}$ [9]. Moreover, we use 1–loop estimates of $c_{\rm V}$, $c_{\rm T}$, $b_{\rm A}$, $b_{\rm P}$, $b_{\rm T}$ [9] as well as of the SF-boundary coefficients $c_{\rm t}$ and $\tilde{c}_{\rm t}$ [11]. The coefficients $\tilde{b}_{\rm A}$ and $\tilde{b}_{\rm V}$ vanish at the tree level and are of order 10^{-2} at 1–loop level [3]. We have hence varied their value in the analysis in the range $-0.2 \div 0.2$ for $\tilde{b}_{\rm A}$ and $-0.1 \div 0.1$ for $\tilde{b}_{\rm V}$, without observing any statistically significant variation in our results.

Our simulation points are listed in table 1: the four values of β correspond to $L/a = 8, 10, 12, 16$. The quoted error on $Lm_{\rm R}$ is purely statistical, due to the negligible uncertainty on $Z_{\rm A}/Z_{\rm P}$. As $Z_{\rm P} \equiv Z_{\rm P}(L_0)$ is known with a relative uncertainty of about 0.5%, the condition (26) is implemented with this precision by adjusting $\mu_{\rm q}$. We correct for small mismatches with the condition eq. (24) using numerical estimates of the $Lm_{\rm R}$–dependence of our observables obtained via some extra simulations at $\beta = 6$. We finally extrapolate our data to the continuum limit assuming convergence with a rate $\propto a^2$. Our fits are shown in figures 1- 4, where only statistical errors are displayed. The results are compatible with $O(a^2)$ deviations from the continuum limit.

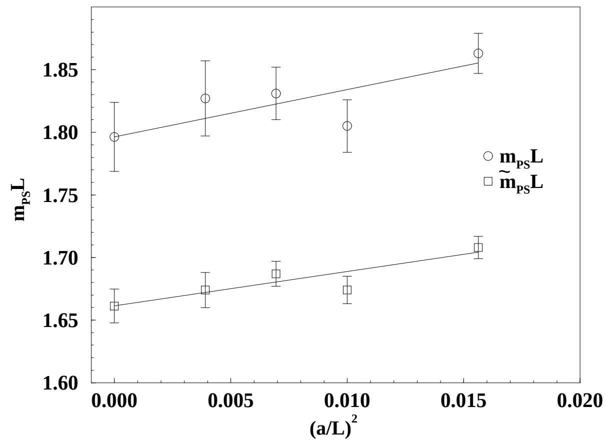

Figure 1. *Scaling of $m_{\rm PS}L$ and $\widetilde{m}_{\rm PS}L$.*

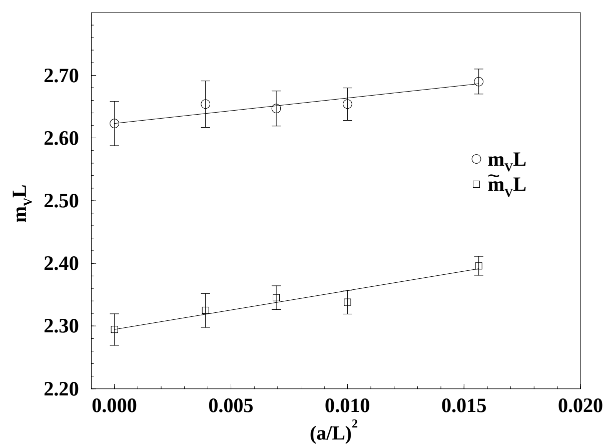

Figure 2. *Scaling of $m_{\rm V}L$ and $\widetilde{m}_{\rm V}L$.*

Because of the finite value of $T \simeq 1.5$ fm, the observables (14)–(21) still depend on the SF boundary action and fields. This induces residual O(a) effects due to the imperfect knowledge of $c_{\rm t}$ and $\tilde{c}_{\rm t}$ and a further coefficient[5] that is associated with O($a\mu_{\rm q}$) effects [3]. Following [7], we have performed a few extra simulations at $\beta = 6$ and $\beta = 6.26$ with values of $c_{\rm t} - 1$ and $\tilde{c}_{\rm t} - 1$ that are about 2 and 10 times, respectively, larger than the 1–loop values. The discrepancies with the previous results are at most about two standard deviations (at $\beta = 6$) and can be considered neg-

[5]Due to $L\mu_{\rm R} = 0.153 \ll 1$, this coefficient was set to its tree level value and never varied.

ligible for the purposes of this study.

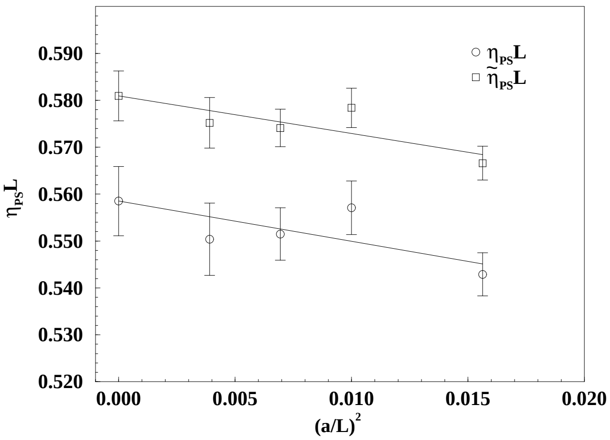

Figure 3. *Scaling of* $\eta_{\rm PS}L$ *and* $\widetilde{\eta}_{\rm PS}L$.

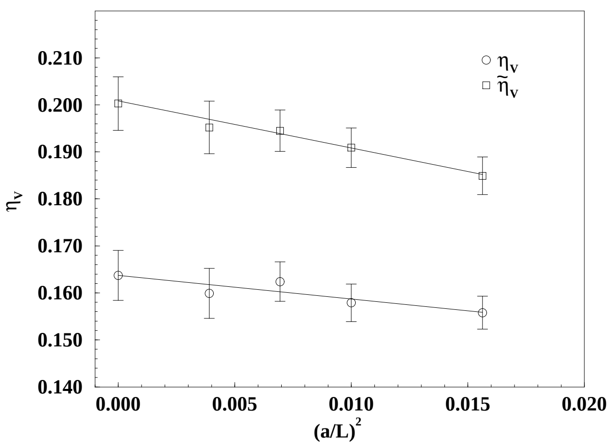

Figure 4. *Scaling of* $\eta_{\rm V}$ *and* $\widetilde{\eta}_{\rm V}$.

In table 2 we compare the estimated continuum limit value of our observables with the value at $\beta = 6$. The deviations from the continuum limit appear to be fairly small and not larger than the ones found in an analogous study at $\mu_{\rm q} = 0$ [7].

5. Conclusions

In the parameter region specified by $\beta \geq 6$, $L\mu_{\rm R} = 0.153 \gg Lm_{\rm R} = 0.020$ and $T = 2L \simeq 1.5$ fm the O(a) improvement programme of tmQCD has been successfully implemented and tested for a few meson observables. The renormalization of the twisted mass parameter is easy in practice, as it can be traced back to the renormalization of the non-singlet pseudoscalar density in the massless theory.

$m_{\rm PS}L$	$m_{\rm V}L$	$\eta_{\rm PS}L$	$\eta_{\rm V}$
1.80(3)	2.62(4)	0.559(7)[1]	0.164(5)[1]
3.7%	2.8%	2.6%	4.8%
$\widetilde{m}_{\rm PS}L$	$\widetilde{m}_{\rm V}L$	$\widetilde{\eta}_{\rm PS}L$	$\widetilde{\eta}_{\rm V}$
1.66(1)	2.29(3)	0.581(5)[1]	0.200(6)[1]
2.7%	4.4%	2.5%	7.7%

Table 2
Continuum limits and deviations from $\beta = 6$. *Errors due to* $Z_{\rm X}$*–uncertainties in square brackets.*

This work is part of the ALPHA collaboration research programme. M. Della Morte and R. Frezzotti thank MURST for support. S. Sint acknowledges support by the European Commission under grant No. FMBICT972442. We thank DESY and INFN for allocating computer time on APE100 machines to this project.

REFERENCES

1. R. Frezzotti, P. A. Grassi, S. Sint and P. Weisz, Nucl. Phys. B (Proc. Suppl.) 83-84 (2000) 941-946.
2. M. Lüscher, S. Sint, R. Sommer and P. Weisz, Nucl. Phys. B478 (1996) 365.
3. R. Frezzotti, P. A. Grassi, S. Sint and P. Weisz, to appear.
4. K. Symanzik, Nucl. Phys. B266 (1983) 187 and 205.
5. M. Lüscher et al., Nucl. Phys. B491 (1997) 323.
6. M. Lüscher, S. Sint, R. Sommer and H. Wittig, Nucl. Phys. B491 (1997) 344.
7. J. Heitger, Nucl. Phys. B557 (1999) 309.
8. S. Sint, Nucl. Phys. B421 (1994) 135.
9. S. Sint and P. Weisz, Nucl. Phys. B502 (1997) 251.
10. M. Lüscher, Commun. Math. Phys. 54, 283 (1977).
11. M. Lüscher, R. Narayanan, P. Weisz and U. Wolff, Nucl. Phys. B384 (1992) 168.
12. M. Guagnelli, R. Sommer and H. Wittig, Nucl. Phys. B535 (1998) 398.
13. S. Capitani, M. Lüscher, R. Sommer and H. Wittig Nucl. Phys. B544 (1999) 669.